High-speed direct space-to-time pulse shaping with 1 ns reconfiguration

Albert Vega,* Daniel E. Leaird, and Andrew M. Weiner

School of Electrical and Computer Engineering, Purdue University, 465 Northwestern Avenue, West Lafayette, Indiana 47907-2035, USA
**Corresponding author: vegaa@purdue.edu*

Received December 9, 2009; revised March 16, 2010; accepted March 17, 2010; posted April 14, 2010 (Doc. ID 121201); published May 5, 2010

In this Letter we demonstrate high-speed direct space-to-time pulse shaping with waveform reconfigurations down to the order of 1 ns. Our pulse shaper implementation incorporates a modified arrayed-waveguide grating structure and an array of optoelectronic reflection modulators. © 2010 Optical Society of America

OCIS codes: 320.5540, 130.3120, 230.4205.

Ultrafast optical pulse shaping is widely employed for applications ranging from ultrafast science to lightwave communications. Most common is the Fourier-transform (FT) pulse shaper in which a spatial light modulator (SLM) manipulates spatially dispersed optical frequency components [1]. Another configuration, particularly relevant for ultrafast parallel-to-serial conversion, is the direct space-to-time (DST) pulse shaper, in which a spatial pattern is directly mapped onto the time-domain electric-field profile [2,3]. Usually the SLMs used in pulse shaping, such as liquid-crystal modulator (LCM) arrays, respond only on a time scale of milliseconds. Microelectro-mechanical systems (MEMS) micromirror arrays have also been used for spatial patterning, e.g., [4]. MEMS micromirrors may have switching times typically in the range of milliseconds down to approximately microseconds [5–7], although, to our knowledge, the fastest devices have not been demonstrated in pulse shaping applications. Thus, the rate at which shaped ultrafast pulses may be reconfigured is significantly limited. Some efforts at faster reconfiguration have been reported. Beam deflection across a two-dimensional LCM in an FT shaper resulted in waveform updates on the order of 100 kHz [8]. Acousto-optic pulse shapers [9] and acousto-optic programmable dispersive filters [10] allow waveform changes at microsecond times but employ a traveling-wave filter pattern that is not suitable for general high repetition rate (oscillator) applications. An integrated waveguide optical phased array providing waveform switching as fast as 30 ns has also been reported [11]. Here, for the first time to our knowledge, we demonstrate waveform reconfiguration as fast as 1 ns, using an array of surface normal semiconductor reflection modulators in a DST pulse shaper configuration based on a modified arrayed waveguide grating (AWG) device.

DST pulse shapers have been reported in bulk optics as well as integrated and partly integrated forms. Originally bulk optic DST shapers were realized using an arrangement consisting of a diffraction grating, lens, and a slit, with a spatial mask placed directly adjacent to the grating [3,12]. At the output of the slit, the mask's spatial pattern is mapped into the time domain according to the transverse delay variation that accompanies the frequency-dependent angular dispersion associated with diffraction from the grating. Later, experiments in which an integrated arrayed waveguide grating chip generated a fixed, high-rate output pulse sequence in response to illumination by a single femtosecond input pulse were explained on the basis of DST pulse shaper action [13]. Using a modified AWG structure, programmable pulse sequence generation is possible [14]. As sketched in Fig. 1, the modified AWG is similar to a conventional AWG [15], but it is cut in half midway through the waveguide array. Retroreflection by an unpatterned mirror placed directly at the output of the chip gives rise to a folded version of a conventional AWG, and standard wavelength demultiplexing properties are observed. However, by using a spatially patterned reflective mask or a reflective modulator array, in conjunction with an input optical pulse shorter than the optical delay difference between waveguides, DST pulse shaping can be achieved. The short input pulse requirement is equivalent to the requirement that the input optical bandwidth should exceed the free spectral range (FSR) of the AWG. Under these conditions the output consists of a sequence of distinct ultrashort pulses, each identified with the round-trip delay of a specific waveguide. Individual pulse intensities correspond to the intensity of light coupled through the specific corresponding waveguide. Hence the temporal envelope of the output intensity may be manipulated by using a mask or modulator array to control the relative intensities reflected back into the various waveguides. This form of integrated DST pulse shaping has interesting application potential as a high-speed parallel-

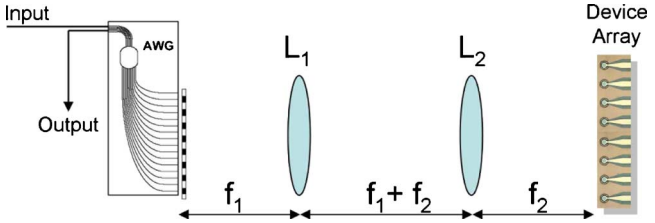

Fig. 1. (Color online) Integrated DST pulse shaper using an AWG, telescope, and modulator array.

to-serial converter [3,16], in which multiple sources of relatively slow (multiple Gbits/s) electrical data would be used to drive an array of reflection modulators, resulting in the serialization of the electrical data onto a much faster optical pulse train.

In the current experiment (Fig. 1), we are using an AWG with a physical guide-to-guide spacing of 150 μm and a single-pass delay increment of 0.8 ps. A mask tilted at an angle near the open face of the AWG blocks every other guide, resulting in a 3.2 ps round-trip delay between the used guides. This exceeds the ~1.2 ps duration of the input pulses used in our experiments. A 6:5 telescope, constructed using two achromatic lenses of focal lengths 60 mm and 50 mm, is used to relay and properly register the output of the waveguide array onto an 8×1 array of modulators, with 150 μm device diameters and 250 μm pitch. Since the AWG has multiple input waveguides, the input and output of the pulse shaper are selected by choosing two of the fiber pigtailed input waveguides. The devices used within the array are asymmetric Fabry–Perot quantum-well surface-normal reflectivity modulators, which can provide good extinction, fast switching, and reasonable optical bandwidth [17,18]. The devices are p-i-n diodes operated in reverse bias and fabricated using III-V semiconductor materials. The device structure (see the inset of Fig. 2) consists of a semi-insulating InP substrate, an eight-period distributed Bragg reflector (DBR) consisting of alternating layers of InAlAs and InAlGaAs (thicknesses 1219 Å and 1138 Å, respectively), 3000 Å n-doped InAlAs, 80 periods of InAlAs/InGaAs quantum wells (QWs) with 74 Å wells and 70 Å barriers serving as the intrinsic layer, 2500 Å p-doped InAlAs, and 300 Å p^+-doped InAlAs serving as a contacting layer. All of the semiconductor layers were grown epitaxially on the substrate, while a quarter wavelength Al_2O_3 antireflection coating was added to the bottom side of the InP to provide low-reflection optical access to the modulators. A metal mirror is deposited via electron beam evaporation onto the top of the semiconductor materials forming the back mirror of the cavity. The front mirror is the buried semiconductor DBR, and the QWs within the cavity serve as an electric-field dependent absorber. This varying absorption causes a change in device reflectivity, which is shown in Fig. 2 along with a plot of the device extinction ratio as an inset. At −15 V bias an extinction ratio over 27 (14 dB) is observed at 1528 nm, with extinction ratio exceeding 10 dB over the range of 1522–1535 nm. The ac response of the device was measured by illuminating the device by a cw source at 1534 nm and varying the frequency of the rf drive signal (superimposed with appropriate dc bias). The estimated 3 dB cutoff frequency is 940 MHz, which is roughly as expected for an RC-limited bandwidth. Faster device performance can be achieved through a reduction in device area, as higher speeds (greater than 20 GHz) have been noted in other similar modulators [18].

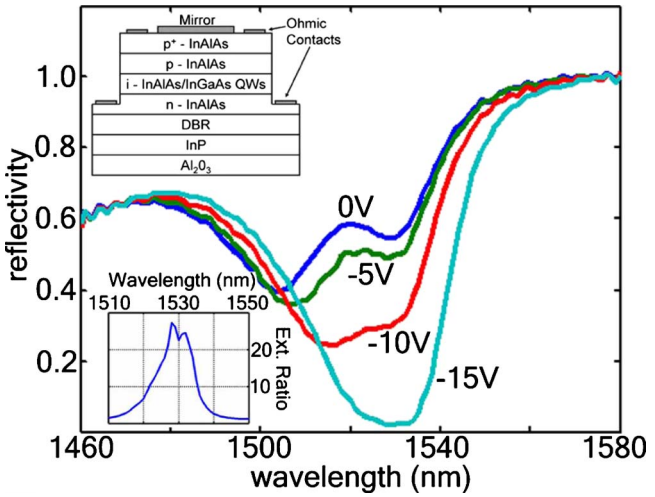

Fig. 2. (Color online) Modulator reflectivity characteristics under bias with extinction ratio (reflectivity of −15 V state divided by the 0 V state) and device structure shown as insets.

The experimental setup, shown in Fig. 3, uses a source that produces ~400 fs pulses FWHM at a repetition rate of 500 MHz. Pulses are derived from a harmonically mode-locked fiber laser at 10 GHz repetition rate, which is connected to a dispersion-decreasing fiber pulse compressor, and then gated using an integrated lithium niobate intensity modulator to reach the lower (500 MHz) repetition rate for our experiments. The source is split into two paths, with one path used as a reference pulse for intensity cross-correlation (XCORR) measurements. The second path is again split, with one branch used to generate the electrical drive signal to the device and the other providing the optical input to the DST shaper. Within the arm to drive the device, there is a motorized optical delay stage, a 1 GHz photodiode (PD) for optical to electrical conversion, a 750 MHz low pass filter (LPF) to smooth the rf signal, and an amplifier with a 12 GHz bandwidth. In these experiments we use a single rf probe, which can be adjusted to contact any one specific device in the array. For the other arm, the signal is sent through an optical bandpass filter which limits the bandwidth to 5 nm centered around 1532 nm, below the optical bandwidth of our modulators, resulting in a 1.2 ps pulse, which is used as input to the pulse shaper. The output of the pulse shaper is amplified by an erbium-doped fiber amplifier (EDFA) and then measured via cross correlation. Both optical paths are dispersion compensated using appropriate lengths of dispersion compensating fiber (DCF).

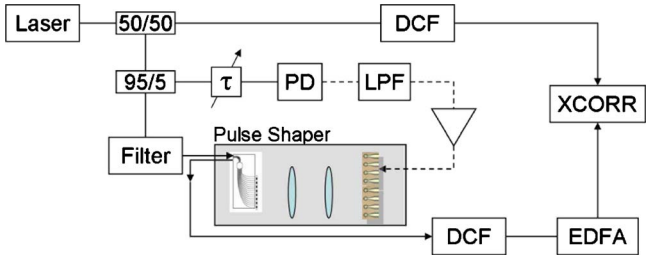

Fig. 3. (Color online) Experimental setup for pulse shaping correlation measurements.

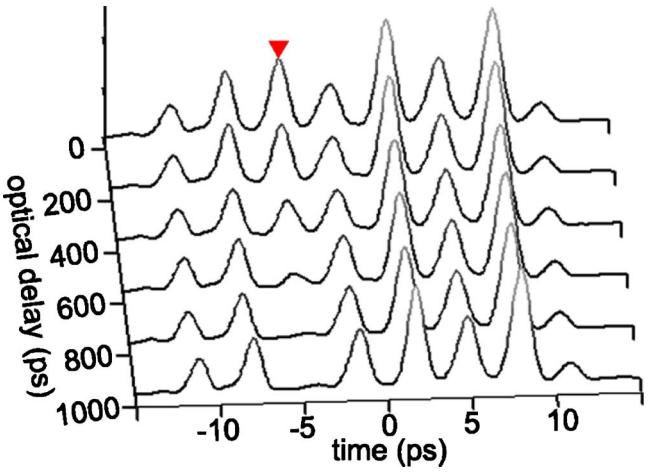

Fig. 4. (Color online) Various cross correlations for varying optical delay relative to 500 MHz electrical drive signal.

To demonstrate control of pulse shaping at rf frequencies, an rf drive signal is applied to a device with a dc reverse bias. Figure 4 shows cross-correlation traces measured for different delays of the rf drive signal. The figure shows the transformation of traces (which indicates the timescale of pulse shaping reconfiguration) as the optical signal is swept through 1 ns (30 cm) of free space optical delay, which corresponds to a π phase change relative to the 500 MHz electrical drive signal. The delay was swept in incremental 200 ps steps, and the overall range was chosen to show a change from a maximum to minimum for a single pulse within the pulse train. These data were taken while the third device in the array was under a −10 V bias, with +18 dBm rf drive power. This bias and rf drive condition was chosen to optimize extinction between the opposing "on/off" states.

Figure 5 shows two examples highlighting the switching between extremes with the same bias and rf power as the previous plot. Figures 5(a) and 5(b) show the intensity cross correlation of the pulse train with the third device in the array driven electrically. In Fig. 5(a) the rf delay is adjusted so that the device is in the "on" state, while in Fig. 5(b) the delay is changed by 1 ns, equal to half of the 2 ns modulation period, so that the device is in the "off" state. When comparing the two plots, the corresponding pulse is suppressed by 11.3 dB. Figures 5(c) and 5(d) show a similar comparison of "on/off" states but while driving the fifth device in the array. The resulting extinction ratio for this device is 10.4 dB under rf operation. These results clearly demonstrate rapid pulse shaper reconfiguration at 1 ns with high extinction.

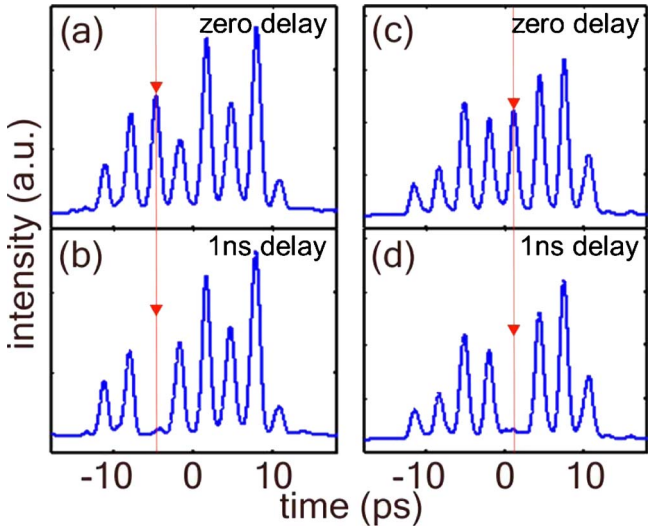

Fig. 5. (Color online) Control of varying devices: (a) output pulse train with a device under dc bias and rf signal in the "on" state; (b) same rf and bias as (a) but device in the "off" state; (c), (d) similar to previous two figures but showing rf modulation of a different device.

In summary, using an array of compound semiconductor reflection modulators and a modified AWG, we were able to demonstrate rapid DST pulse shaping updating at 1 ns with >10 dB extinction ratios for both dc and rf functionality. By using smaller devices for reduced capacitance, higher-speed performance should be possible, enabling reconfiguration at 10 GHz rates relevant for telecommunications applications.

References

1. A. M. Weiner, Rev. Sci. Instrum. **71**, 1929 (2000).
2. D. E. Leaird and A. M. Weiner, Opt. Lett. **24**, 853 (1999).
3. D. E. Leaird and A. M. Weiner, IEEE J. Quantum Electron. **37**, 494 (2001).
4. A. Krishnan, M. Knapczyk, L. Grave de Peralta, A. A. Bernussi, and A. Temkin, IEEE Photonics Technol. Lett. **17**, 1959 (2005).
5. A. Tuantranont, T. Lomas, and V. M. Bright, Proc. SPIE **5276**, 221 (2004).
6. L. J. Hornbeck, in *International Electron Devices Meeting, IEDM* (2007), pp. 17–24.
7. G. N. Nielson, R. H. Olsson, P. R. Resnick, and O. B. Spahn, in *Conference on Lasers and Electro-Optics* (Optical Society of America, 2007), paper CMP2.
8. E. Frumker and Y. Silberberg, Opt. Lett. **32**, 1384 (2007).
9. C. W. Hillegas, J. X. Tull, D. Goswami, D. Strickland, and W. S. Warren, Opt. Lett. **19**, 737 (1994).
10. F. Verluise, V. Laude, Z. Cheng, Ch. Spielmann, and P. Tournois, Opt. Lett. **25**, 575 (2000).
11. E. Frumker, E. Tal, Y. Silberberg, and D. Majer, Opt. Lett. **30**, 2796 (2005).
12. C. Froehly, B. Colombeau, and M. Vampouille, Prog. Opt. **20**, 65 (1983).
13. D. E. Leaird, A. M. Weiner, S. Shen, A. Sugita, S. Kamei, M. Ishii, and K. Okamoto, Opt. Quantum Electron. **33**, 811 (2001).
14. D. E. Leaird and A. M. Weiner, Opt. Lett. **29**, 1551 (2004).
15. K. Okamoto, Opt. Quantum Electron. **31**, 107 (1999).
16. J. D. McKinney, D.-S. Seo, and A. M. Weiner, IEEE J. Quantum Electron. **39**, 1635 (2003).
17. R. H. Yan, R. J. Simes, and L. A. Coldren, Appl. Phys. Lett. **55**, 1946 (1989).
18. S. J. B. Yoo, R. Bhat, C. Caneau, J. Gamelin, M. A. Koza, and T. P. Lee, in *Lasers and Electro-Optics Society Annual Meeting* (Optical Society of America, 1995), Vol. 8, paper ThK5.